Inorg. Chem. **2005**, *44*, 2619–2627

A Platinum Acetylide Polymer with Sterically Demanding Substituents: Effect of Aggregation on the Triplet Excited State

Xiaoming Zhao, Thomas Cardolaccia, Richard T. Farley, Khalil A. Abboud, and Kirk S. Schanze*

Department of Chemistry, University of Florida, P.O. Box 117200, Gainesville, Florida 32601-7200

Received July 30, 2004

The effect of interchain interaction on the triplet excited state is explored in two Pt–acetylide polymers of the type [–*trans*-Pt(PBu$_3$)$_2$–C≡C–Ar–C≡C–]$_n$, where Ar is either 1,4-phenylene or is based on the pentiptycene unit (polymers **2** and **3**, respectively). To explore the effect of interchain interaction in Pt–acetylide materials, the optical properties of parent polymer **2** are compared with those of polymer **3** in which interchain interaction is precluded by the sterically bulky pentiptycene moiety. Insight into the effect of the pentiptycene unit on packing in the solid state comes from the X-ray structure of monomer **1b**, Ph–C≡C–[*trans*-Pt(PBu$_3$)$_2$]–C≡C–Ar–C≡C–[*trans*-Pt(PBu$_3$)$_2$]–C≡C–Ph. Spectroscopic studies indicate that weak phosphorescence emission from an interchain aggregate is observed from parent polymer **2**, both in solution and in the solid state. By contrast, the photophysics of **3** is dominated by the intrachain triplet exciton. Interestingly, the phosphorescence emission of polymer **3** in the solid state is nearly superimposable with that of a single crystal of monomer **1b**, suggesting that the solid polymer experiences an environment that is similar to that of the monomer in the crystal.

Introduction

Conjugated polymers are promising candidates for a variety of applications including chemo- and biosensing,[1] electroluminescence,[2−4] and optical limiting.[5,6] Most applications of conjugated polymers require that the materials be used in a solid-state format such as a thin film. It is well-known that the optical and electronic properties of conjugated molecules in the solid state differ significantly from those observed for the same materials in dilute solution or dispersed at low concentration into a nonconjugated host polymer.[7,8] For example, in the solid state, aggregates dominate the photophysics of most conjugated polymers.[9,10] The topic has been investigated thoroughly for polymers such as poly(phenylene vinylene) and poly(phenylene ethynylene) (PPV and PPE, respectively), which exhibit fluorescence from the singlet exciton. In particular, the fluorescence of thin films of PPV- and PPE-type polymers is red-shifted and broadened relative to the fluorescence from the same materials in dilute solution.[8,11−15] The red-shifted fluorescence is attributed to an excimer-like state that results from π-stacking of aromatic residues in the solid. This model for aggregate formation in the solid materials is supported by the fact that the optical properties of conjugated polymers that are decorated with sterically demanding groups such as dendrimers[16,17] or pentiptycene[12,13,18] are nearly the same in solution and in the solid state.

* Author to whom correspondence should be addressed. E-mail: kschanze@chem.ufl.edu. Tel: 352-392-9133. Fax: 352-392-2395.

(1) McQuade, D. T.; Pullen, A. E.; Swager, T. M. *Chem. Rev.* **2000**, *100*, 2537−2574.
(2) Burroughes, J. H.; Bradley, D. D. C.; Brown, A. R.; Marks, R. N.; Mackay, K.; Friend, R. H.; Burn, P. L.; Holmes, A. B. *Nature* **1990**, *347*, 539−541.
(3) Braun, D.; Heeger, A. J. *App. Phys. Lett.* **1991**, *58*, 1982−1984.
(4) Friend, R. H.; Gymer, R. W.; Holmes, A. B.; Burroughes, J. H.; Marks, R. N.; Taliani, C.; Bradley, D. D. C.; Dos Santos, D. A.; Brédas, J. L.; Lögdlund, M.; Salaneck, W. R. *Nature* **1999**, *397*, 121−128.
(5) Spangler, C. W. *J. Mater. Chem.* **1999**, *9*, 2013−2020.
(6) McKay, T. J.; Bolger, J. A.; Staromlynska, J.; Davy, J. R. *J. Chem. Phys.* **1998**, *108*, 5537−5541.
(7) Yan, M.; Rothberg, L. J.; Kwock, E. W.; Miller, T. M. *Phys. Rev. Lett.* **1995**, *75*, 1992−1995.
(8) Rothberg, L. J.; Yan, M.; Papadimitrakopoulos, F.; Galvin, M. E.; Kwock, E. W.; Miller, T. M. *Synth. Met.* **1996**, *80*, 41−58.
(9) Lemmer, U.; Heun, S.; Mahrt, R. F.; Scherf, U.; Hopmeier, M.; Siegner, U.; Göbel, E. O.; Müllen, K.; Bässler, H. *Chem. Phys. Lett.* **1995**, *240*, 373−378.
(10) Jenekhe, S. A.; Osaheni, J. A. *Science* **1994**, *265*, 765−768.
(11) Samuel, I. D. W.; Rumbles, G.; Collison, C. J.; Moratti, S. C.; Holmes, A. B. *Chem. Phys.* **1998**, *227*, 75−82.
(12) Williams, V. E.; Swager, T. M. *Macromolecules* **2000**, *33*, 4069−4073.
(13) Yang, J.-S.; Swager, T. M. *J. Am. Chem. Soc.* **1998**, *120*, 11864−11873.
(14) Halkyard, C. E.; Rampey, M. E.; Kloppenburg, L.; Studer-Martinez, S. L.; Bunz, U. H. F. *Macromolecules* **1998**, *31*, 8655−8659.
(15) Miteva, T.; Palmer, L.; Kloppenburg, L.; Neher, D.; Bunz, U. H. F. *Macromolecules* **2000**, *33*, 652−654.
(16) Sato, T.; Jiang, D.-L.; Aida, T. *J. Am. Chem. Soc.* **1999**, *121*, 10658−10659.

10.1021/ic048961s CCC: $30.25
Published on Web 03/11/2005

Although a great deal is known about the properties of the singlet state in conjugated polymers and how its properties are influenced by aggregation, comparatively less is known about the lowest triplet state.[19−22] This is clearly an important issue, since the triplet exciton plays an important role in applications such as electroluminescence,[23,24] optical limiting,[25] and luminescent sensors.[26,27] A factor that limits the ability to investigate the properties of the triplet state in all-organic conjugated materials is the fact that phosphorescence is rarely observed.[28] As a consequence, emission spectroscopy cannot be used to examine how the properties of the triplet state are influenced by factors such as chain structure and medium. A number of recent investigations have demonstrated that platinum(II)−acetylide-based polymers, which are structurally analogous to poly(phenylene ethynylene)s, have high intersystem crossing efficiencies and display phosphorescence from the triplet exciton at room temperature, both in solution and in the solid state.[29−31] Because of this property, Pt−acetylide polymers and oligomers provide a unique opportunity to use spectroscopy to explore factors that influence the triplet exciton in π-conjugated systems. Specifically, work to date on this class of materials has shown conclusively that the triplet exciton is less delocalized than the singlet,[28,30,32] that the energy gap law for nonradiative decay holds for a series of Pt−acetylide-based polymers and oligomers,[33] and that the singlet−triplet branching ratio in electroluminescent devices may be influenced by the degree of conjugation in the material.[34]

In the present investigation, we have characterized the optical properties of a series of Pt−acetylide-based oligomers and polymers that contain the bulky pentiptycene unit to disrupt interchain interactions in the solid-state materials. As noted above, Swager and co-workers developed the iptycene moiety as a sterically demanding unit to disrupt interchain aggregates in PPE-type polymers.[12,13,18] In the present investigation we have applied their strategy to explore the influence of aggregates on the triplet state in π-conjugated polymers. The Pt−acetylide materials that are the focus of this study display strong phosphorescence from the triplet exciton in the solid state, affording the opportunity to explore how aggregation influences the properties of the triplet state. Comparison of the PL spectra of an iptycene-containing monomer and polymer with those of a corresponding phenylene-based polymer shows that aggregation in the phenylene system clearly affects the triplet state. The effects of aggregation are discussed in terms of possible interaction mechanisms, including $\pi-\pi$ stacking of the phenylene units and the introduction of low-lying excitations derived from dσ* → pσ/π* MMCT (metal−metal to ligand charge transfer)[35,36] configurations which arise from interchain Pt−Pt interactions.

Experimental Section

General Synthetic Procedures and Source of Starting Materials. All chemicals used for synthesis were of reagent grade and used without purification unless noted. Reactions were carried out under an argon atmosphere with freshly distilled solvents, unless otherwise noted. ^{1}H, ^{13}C, and ^{31}P NMR spectra were recorded on either a Varian Gemini 300 or Mercury 300 spectrometer, and chemical shifts are reported in ppm relative to TMS. *cis*-Dichlorobis(tri-*n*-butylphosphine)platinum(II),[37] 1,4-diethynylbenzene,[32] and polymer **2**[31] were prepared by literature methods. (GPC analysis of polymer **2** gave M_n = 11 400 g mol^{-1}, M_w = 32 100 g-mol^{-1}, and PDI = 2.81. The ^{1}H NMR spectrum of the polymer is provided as Supporting Information.) The diethynyl iptycene compound (6,13-diethynyl-5,7,12,14-tetrahydro-5,14[1′,2′]:7,12[1″,2″]dibenzopentacene, CAS Registry No. 214461-10-6, herein referred to as compound **4**) was prepared as described by Yang and Swager.[13] The molecular weights of the polymers were determined on a GPC column with a Beckman Instruments Spectroflow 757 absorbance detector at 270 nm and a flow rate of 1.0 mL/min, using THF as the eluent and two PLgel 5 μm MIXED-D columns (Polymer Laboratories). Molecular weights are reported relative to polystyrene standards.

Complex 1a. Diethynyl iptycene **4** (47.6 mg, 0.1 mmol) was dissolved in toluene/piperidine (4:1, 10 mL), and CuI (1 mg) was added. The mixture was degassed for 20 min, whereupon *cis*-dichlorobis(tri-*n*-butylphosphine)platinum(II) (200 mg, 0.3 mmol) was added quickly and the reaction mixture was stirred overnight at 70 °C. The solvents were removed under reduced pressure, and the residue was purified by column chromatography on silica. A white solid (140 mg, 80%) was collected. ^{1}H NMR (300 MHz, $CDCl_3$): δ 0.89 (t, J = 7.5 Hz, 36H), 1.39−1.52 (m, 24H),

(17) Setayesh, S.; Grimsdale, A. C.; Weil, T.; Enkelmann, V.; Müllen, K.; Meghdadi, F.; List, E. J. W.; Leising, G. *J. Am. Chem. Soc.* **2001**, *123*, 946−953.
(18) Zhu, Z.; Swager, T. M. *Org. Lett.* **2001**, *3*, 3471−3474.
(19) Walters, K. A.; Ley, K. D.; Schanze, K. S. *Chem. Commun.* **1998**, *10*, 1115−1116.
(20) Burrows, H. D.; Seixas de Melo, J.; Serpa, C.; Arnaut, L. G.; Monkman, A. P.; Hamblett, I.; Navarathnam, S. *J. Chem. Phys.* **2001**, *115*, 9601−9606.
(21) Monkman, A. P.; Burrows, H. D.; Hamblett, I.; Navarathnam, S.; Svensson, M.; Andersson, M. R. *J. Chem. Phys.* **2001**, *115*, 9046−9049.
(22) Monkman, A. P.; Burrows, H. D.; Hartwell, L. J.; Horsburgh, L. E.; Hamblett, I.; Navaratnam, S. *Phys. Rev. Lett.* **2001**, *86*, 1358−1361.
(23) Baldo, M. A.; O'Brien, D. F.; You, Y.; Shoustikov, A.; Sibley, S.; Thompson, M. E.; Forrest, S. R. *Nature* **1998**, *395*, 151−153.
(24) Sandee, A. J.; Williams, C. K.; Evans, N. R.; Davies, J. E.; Boothby, C. E.; Köhler, A.; Friend, R. H.; Holmes, A. B. *J. Am. Chem. Soc.* **2004**, *126*, 7041−7048.
(25) Perry, J. W. In *Nonlinear Optics of Organic Molecules and Polymers*; Nalwa, H. S., Miyata, S., Eds.; CRC Press: Boca Raton, FL, 1997; pp 813−840.
(26) Carraway, E. R.; Demas, J. N.; DeGraff, B. A.; Bacon, J. R. *Anal. Chem.* **1991**, *63*, 337−342.
(27) Mills, A. *Platinum Met. Rev.* **1997**, *41*, 115−127.
(28) Köhler, A.; Wilson, J. S.; Friend, R. H.; Al-Suti, M. K.; Khan, M. S.; Gerhard, A.; Bässler, H. *J. Chem. Phys.* **2002**, *116*, 9457−9463.
(29) Wittmann, H. F.; Friend, R. H.; Khan, M. S.; Lewis, J. *J. Chem. Phys.* **1994**, *101*, 2693−2698.
(30) Beljonne, D.; Wittmann, H. F.; Köhler, A.; Graham, S.; Younus, M.; Lewis, J.; Raithby, P. R.; Khan, M. S.; Friend, R. H.; Brédas, J. L. *J. Chem. Phys.* **1996**, *105*, 3868−3877.
(31) Wilson, J. S.; Köhler, A.; Friend, R. H.; Al-Suti, M. K.; Al-Mandhary, M. R. A.; Khan, M. S.; Raithby, P. R. *J. Chem. Phys.* **2000**, *113*, 7627−7634.
(32) Liu, Y.; Jiang, S.; Glusac, K.; Powell, D. H.; Anderson, D. F.; Schanze, K. S. *J. Am. Chem. Soc.* **2002**, *124*, 12412−12413.
(33) Wilson, J. S.; Chawdhury, N.; Al-Mandhary, M. R. A.; Younus, M.; Khan, M. S.; Raithby, P. R.; Köhler, A.; Friend, R. H. *J. Am. Chem. Soc.* **2001**, *123*, 9412−9417.
(34) Wilson, J. S.; Dhoot, A. S.; Seeley, A. J. A. B.; Khan, M. S.; Köhler, A.; Friend, R. H. *Nature* **2001**, *413*, 828−831.
(35) Roundhill, D. M.; Gray, H. B.; Che, C.-M. *Acc. Chem. Res.* **1989**, *22*, 55−61.
(36) Yam, V. W.-W. *Acc. Chem. Res.* **2002**, *35*, 555−563.
(37) Kauffman, G. B.; Teter, L. A. *Inorg. Synth.* **1963**, *7*, 245−249.

1.63−1.78 (m, 24H), 2.08−2.20 (m, 24H), 5.93 (s, 4H), 6.82−6.89 (dd, $J_1 = 3.0$ Hz, $J_2 = 3.3$ Hz, 8H), 7.18−7.26 (dd, $J_1 = 3.3$ Hz, $J_2 = 3.6$ Hz, 8H). ^{13}C NMR (75 MHz, $CDCl_3$): δ 13.83, 21.92, 22.15, 22.36, 24.15, 24.24, 24.32, 26.34, 52.15, 89.27, 96.52, 117.11, 123.19, 124.51, 141.70, 146.08. ^{31}P NMR ($CDCl_3$, 121 MHz): δ 8.25 ($J = 2375.8$ Hz). Anal. Calcd for $C_{86}H_{128}Cl_2P_4Pt_2$: C, 59.13; H, 7.39. Found: C, 58.92; H, 7.49.

Complex 1b. Complex **1a** (106 mg, 0.061 mmol) was dissolved in toluene/piperidine (2:1, 3 mL), and CuI (1 mg) was added. The mixture was degassed for 20 min with argon, whereupon phenylacetylene (12.44 mg, 0.122 mmol) was added quickly and the reaction mixture was stirred overnight at room temperature. The solvents were removed under reduced pressure, and the residue was purified by column chromatography on silica. A yellow solid (95 mg, 83%) was collected. ^{1}H NMR (300 MHz, $CDCl_3$, spectrum shown in Supporting Information): δ 0.91 (t, $J = 7.2$ Hz, 36 H), 1.41−1.55 (m, 24 H), 1.65−1.81 (m, 24H), 2.19−2.37 (m, 24H), 5.98 (s, 4H), 6.81−6.85 (m, 8H), 7.16−7.19 (m, 2H), 7.20−7.24 (m, 12H), 7.32−7.38 (m, 4H). ^{31}P NMR (121 MHz, $CDCl_3$): δ 4.63 ($J = 2362.0$ Hz). Anal. Calcd for $C_{102}H_{138}Cl_2P_4Pt_2$: C, 65.23; H, 7.41. Found: C, 64.58; H, 7.58.

Polymer 3. To a mixture of *cis*-dichlorobis(tri-*n*-butylphosphine)-platinum(II) (210 mg, 0.31 mmol) and diethynyl iptycene **4** (210 mg, 0.31 mmol) in toluene/*i*-Pr_2NH (3:1, 10 mL), CuI (10 mg, 0.05 mmol) was added quickly, and the resulting solution was degassed for 20 min with argon. The yellow solution was stirred at 65 °C overnight. All volatile components were removed under reduced pressure, and the residue was dissolved in dichloromethane and filtered through a short alumina column. After removal of solvent under reduced pressure, a yellow solid was collected. Further purification was accomplished by precipitating the polymer solution in dichloromethane from methanol. Polymer **3** (260 mg, 77%) was obtained as a yellow solid. ^{1}H NMR (300 MHz, $CDCl_3$, spectrum shown in Supporting Information): δ 0.79−0.94 (br m, 18 H), 1.36−1.58 (br m, 12H), 1.60−1.94 (br m, 12H), 2.21−2.49 (br m, 12H), 6.00−6.19 (br m, 4H), 6.82−7.03 (br m, 8H), 7.59−7.82 (br m, 8H). ^{31}P NMR (121 MHz, $CDCl_3$): δ 8.28 ($J = 2382.8$ Hz). GPC (polystyrene standards): $M_n = 4350$ g mol^{-1}; $M_w = 5850$ g mol^{-1}; PDI = 1.34.

Photophysical Measurements. Corrected steady-state emission measurements were conducted on a SPEX F-112 fluorescence spectrophotometer. Sample concentrations were adjusted to produce optically dilute solutions ($A_{max} < 0.20$, $c \approx 1$ μM) and optically thick films ($A_{max} \approx 1.0$). Fluorescence quantum yields were determined according to the optically dilute method described by Demas and Crosby, with the quantum yield being computed according to eq 14 in their paper.[38] Solutions of perylene and 9,10-dicyanoanthracene in ethanol were used in parallel as actinometers ($\Phi_F = 0.89$ for both in ethanol). Steady-state absorption spectra were recorded on a Varian Cary 100 dual-beam spectrophotometer. Transient absorption measurements were conducted on an apparatus which has been described elsewhere.[39] Excitation was effected with the 3rd harmonic of a Nd:YAG laser ($\lambda = 355$ nm, 10 ns fwhm, 10 mJ pulse^{-1}). Sample concentrations were adjusted so that $A \approx 0.8$ at 355 nm. Time-resolved emission measurements were recorded on an apparatus consisting of a Quanta Ray GCR Series Nd:YAG laser as a source (3rd harmonic, $\lambda = 355$ nm, 10 ns fwhm) with time-resolved detection provided by an intensified CCD detector (Princeton Instruments, PI-MAX iCCD) coupled to an Acton SpectraPro 150 spectrograph.

(38) Demas, J. N.; Crosby, G. A. *J. Phys. Chem.* **1971**, *75*, 991−1024.
(39) Wang, Y.; Schanze, K. S. *Chem. Phys.* **1993**, *176*, 305.

Table 1. Crystallographic Parameters for **1b**

empirical formula	$C_{102}H_{138}P_2Pt$
temp	173(2) K
cryst system	monoclinic
space group	*C*2/*c*
unit cell dimens	$a = 35.608(2)$ Å, $\alpha = 90°$ $b = 13.7399(8)$ Å, $\beta = 124.806(2)°$ $c = 23.5629(14)$ Å, $\gamma = 90°$
V	9465.6(10) Å^3
Z	4
cryst size	$0.24 \times 0.20 \times 0.19$ mm^3
data/restraints/params	10 650/0/469
goodness-of-fit on F^2	1.031
final R indices [$I > 2\sigma(I)$][a]	R1 = 0.0521, wR2 = 0.1053 [6994]
R indices (all data)[a]	R1 = 0.0914, wR2 = 0.1218

[a] $R1 = \Sigma(||F_o| - |F_c||)/\Sigma|F_o|$. $wR2 = [\Sigma[w(F_o^2 - F_c^2)^2]/\Sigma[w(F_o^2)^2]]^{1/2}$. $S = [\Sigma[w(F_o^2 - F_c^2)^2]/(n - p)]^{1/2}$. $w = 1/[\sigma^2(F_o^2) + (mp)^2 + np]$, $p = [\max(F_o^2,0) + 2F_c^2]/3$, m and n are constants.

X-ray Structure Determination of 1b. Data were collected at 173 K on a Siemens SMART PLATFORM equipped with A CCD area detector and a graphite monochromator utilizing Mo Kα radiation ($\lambda = 0.710\ 73$ Å). Cell parameters were refined using up to 8192 reflections. A full sphere of data (1850 frames) was collected using the ω-scan method (0.3° frame width). The first 50 frames were remeasured at the end of data collection to monitor instrument and crystal stability (maximum correction on I was <1%). Absorption corrections by integration were applied on the basis of the measured indexed crystal faces.

The structure was solved by the direct methods in SHELXTL6[40] and refined using full-matrix least squares. The non-H atoms were treated anisotropically, whereas the hydrogen atoms were calculated in ideal positions and were riding on their respective carbon atoms. The complexes are located on centers of inversion; thus, the asymmetric unit consists of a half complex. All of three butyl groups around the P atom are disordered, and each was refined in two parts with their site occupation factors dependently refined. Crystallographic parameters are listed in Table 1.The atomic numbering is shown in Chart 1.

Results and Discussion

Polymer and Monomer Structures. The focus of this investigation is to determine the effect of interchain interaction on the spectroscopic properties of the triplet excited state in Pt−acetylide-based π-conjugated polymers. To address this problem, we sought to compare the optical properties of the "parent" polymer, **2**, with those of the iptycene-substituted polymer **3** (see Chart 2 for structures). Polymer **2** features a repeat consisting of the *trans*-$Pt(PBu_3)_2$ unit alternating with 1,4-diethynylbenzene. Due to the square-planar geometry around the Pt(II) center, in the solid-state polymer **2** can adopt an "all planar" conformation in which strong interchain interactions might be expected. However, due to the significant steric constraints imposed by the iptycene unit in polymer **3**, strong interchain interaction is not expected for this material in the solid state.[12,13] To a first-order approximation, the electronic structure with respect to the π-conjugated electronic system is the same in the two polymers. However, as discussed in more detail below, due to the bulky iptycene unit, there are likely to be differences in conformation of the monomer units with respect to the

(40) Sheldrick, G. M. *SHELXTL6*; Bruker-AXS: Madison, WI, 2000.

Chart 1. Atomic Numbering for **1b**

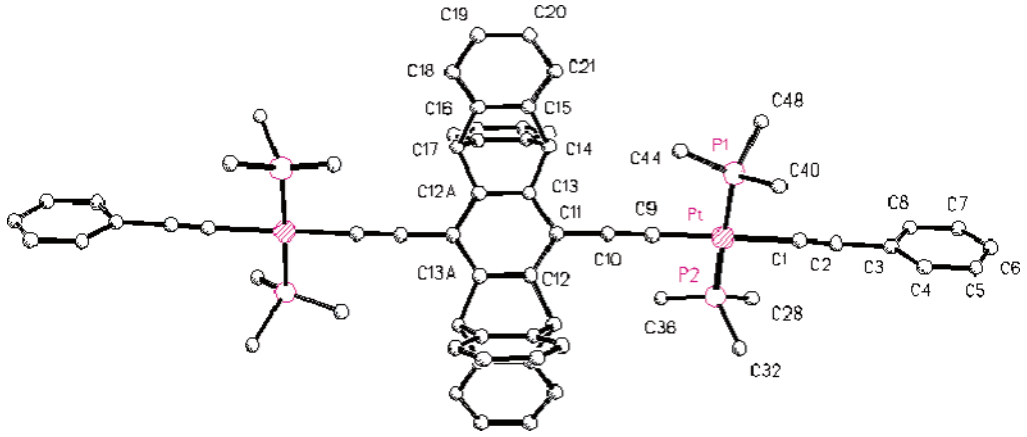

Chart 2

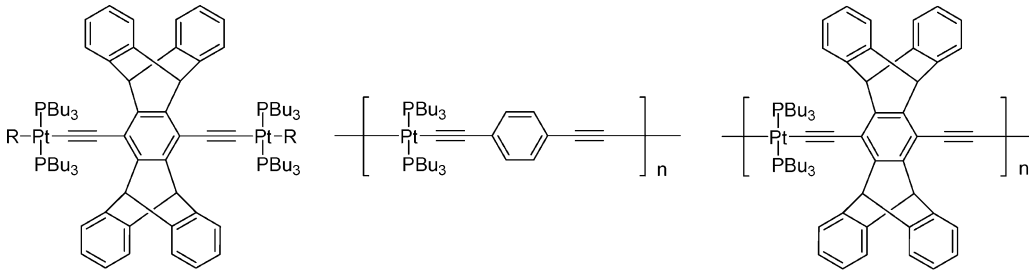

1a: R = Cl
1b: R = phenylacetylene

2 **3**

polymer backbone in **2** and **3**, and these differences may result in measurable differences in the optical properties of the two polymers.

To provide more information concerning the structure of the iptycene unit on the Pt−acetylides, we also prepared two model monomers, **1a**,**b**. Fortunately, these materials were crystalline solids, and as a result it was possible to deduce their structures by X-ray crystallography (see below).

X-ray Crystallography. The X-ray crystal structures of compounds **1a**,**b** were elucidated. The thermal ellipsoid plot for **1b** is shown in Figure 1 (top), while the corresponding plot for **1a** is included as Supporting Information. Detailed crystal structure data for **1a**,**b** is provided as CIF files in Supporting Information, and selected structural parameters for **1b** are listed in Table 2. Compound **1b** crystallizes in a monoclinic crystal system and belongs to the *C*2/*c* space group. As expected, the PtP_2C_2 unit is approximately square planar, with a P−Pt−C bond angle of 89°.

Close inspection of the data in Table 2 reveals that there is asymmetry with respect to the Pt−acetylide bonding. Specifically, the bond lengths on the terminal phenyl acetylene groups alternate strongly in distance, i.e., Pt−C1 is long (2.10 Å), C1−C2 is short (1.02 Å), and C2−C3 is long (1.52 Å). By contrast, there is less bond length alternation in the central acetylides: Pt−C9 (1.98 Å); C9−C10 (1.22 Å); C10−C11 (1.42 Å). While this effect could signal stronger d → π^* back-bonding from Pt to the central acetylide ligand, the C9−C10 bond is only slightly longer than the C≡C bond in the free diethynyl iptycene ligand (as the $-Si(CH_3)_3$ derivative, the bond length is 1.215 Å, crystal structure reported by Yang and Swager).[13] Thus, the difference in C≡C bond lengths in **1b** may be dictated by the electronic properties of the iptycene unit, which is likely to be more electron rich than a phenyl group lacking alkyl substituents.

Figure 1 (bottom) illustrates an end-on view of **1b** in the crystal, with the hydrogens removed and the butyl chains

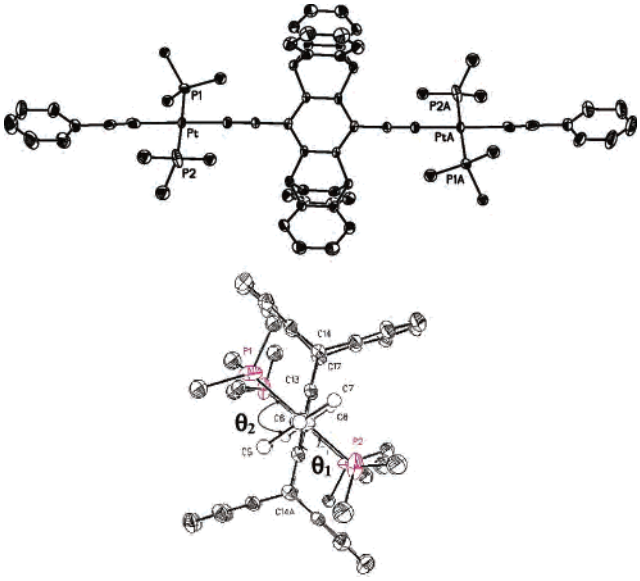

Figure 1. Top: ORTEP diagram of **1b**. Bottom: X-ray ORTEP diagram of **1b** viewed along the Pt−acetylide bond axis (crystallographic *a*-axis). Only the first carbon atoms of the butyl groups on the phosphine ligands are shown for clarity. (Note that angles θ_1 and θ_2 are defined in the diagram; see text for a discussion.)

Table 2. Selected Bond Lengths and Angles for Complex **1b**[a]

bond	length/Å	bond angle	angle/deg
Pt−P1	2.291(2)	C1−Pt−C9	179.3(3)
Pt−P2	2.296(2)	P1−Pt−P2	178.06(7)
Pt−C1	2.104(7)	C1−Pt−P1	89.6(2)
Pt−C9	1.982(5)	C1−Pt−P2	88.7(2)
C1−C2	1.025(9)	C1−C2−C3	176.8(10)
C9−C10	1.221(7)	C9−C10−C11	178.8(7)
C2−C3	1.527(10)		
C10−C11	1.427(7)		

[a] Atomic numbering system is shown in Chart 1 (see Experimental Section).

on the phosphine ligands truncated to improve clarity. This view allows one to visualize the orientation of the planes defined by the PtP_2C_2 units relative to the planes defined by the iptycene phenylene unit and the terminal phenylene rings (θ_1 and θ_2, respectively; see Figure 1, bottom). Interestingly, the two terminal phenylenes lie in the same plane and the two PtP_2C_2 units are in the same plane. However, each of these sets of planar units is twisted relative to one another. Specifically, the angle between the plane defined by the iptycene phenylene and the PtP_2C_2 units is $\theta_1 = 60 \pm 1°$, whereas the angle between the PtP_2C_2 units and the terminal phenylenes is $\theta_2 = 77 \pm 1°$. The fact that these planes are twisted relative to one another is consistent with observations on other Pt−acetylide complexes which have been studied by X-ray crystallography, where the planes are twisted by ≈60°.[41,42] It is likely that steric interactions between the PBu_3 ligands and the iptycene unit have an influence on the relative orientation of the PtP_2C_2 units and the iptycene phenylene ring. Computer-aided molecular modeling (Chem 3D, version 7.0) suggests that rotation of the units with respect to the Pt−acetylide chain axis is limited by these steric interactions to a range such that the planes defined by the PtP_2C_2 and iptycene phenylene units remain twisted by >60°. It is important to note that, despite the twisting, the π-electron systems of the individual units of the Pt−acetylide chain are conjugated via interactions with the (filled) d_{xy} and/or d_{xz} orbitals on the Pt centers.[43]

A view of the unit cell packing diagram for **1b** is shown in Figure 2. It is quite evident from this diagram that, due to the large steric constraints imposed by the PBu_3 groups (not shown) and the iptycene units, the Pt−acetylide chains are well-separated in the crystal. The separation distance between the chains is exactly half of the *c*-axis length, or 11.782(1) Å. This distance is sufficiently large so as to preclude any significant $\pi-\pi$ or $d-\pi$ interactions between adjacent monomers in the crystal. Thus, it is expected that the optical properties of the molecules in the crystal should be very similar to those for the isolated molecules in solution.

Photophysics in Solution. The left panel of Figure 3 compares absorption spectra for compound **1b** and polymers **2** and **3** in THF solution. The spectra of all three materials

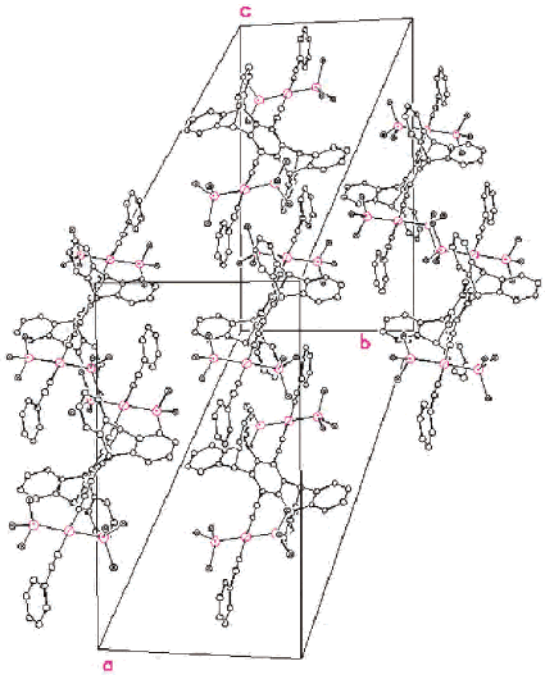

Figure 2. Unit cell packing diagram for compound **1b**. Only the first carbon atom of each butyl chain on the phosphine ligands is shown for clarity.

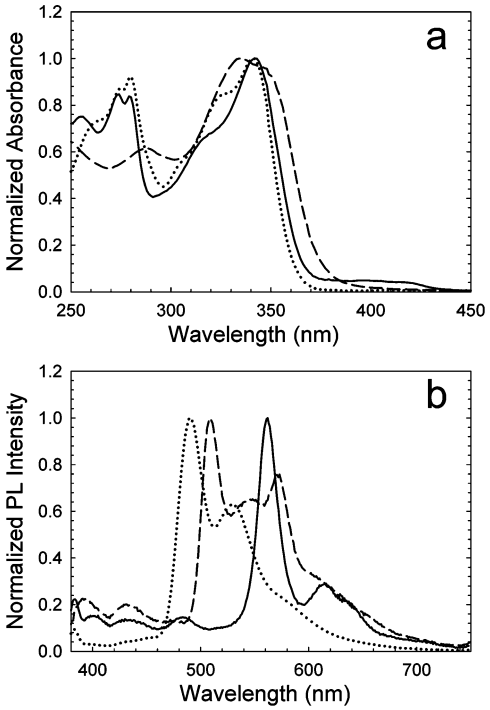

Figure 3. Normalized absorption (a) and photoluminescence (b) spectra of polymer **2** (- - -), polymer **3** (—), and monomer **1b** (···) in THF solution. Photoluminescence measurements were carried out on argon-deoxygenated solutions. Concentrations: **2**, 0.5 μM; **3**, 1.0 μM; **1b**, 5 μM.

are dominated by a strong and relatively broad band in the near-UV region (≈350 nm), which is due to the long-axis polarized π,π^* transition of the Pt−acetylide chromophore. Although the spectra are similar, close inspection reveals quantitative differences among them. In particular, monomer **1b** and polymer **3** feature an additional absorption band in the 270−280 nm region arising from the nonconjugated aryl

(41) Davy, J.; Gunter, M. E.; Tiekink, E. R. T. *Z. Kristallogr.* **1998**, *213*, 483−486.
(42) Haskins-Glusac, K.; Ghiviriga, I.; Abboud, K. A.; Schanze, K. S. *J. Phys. Chem. B* **2004**, *108*, 4969−4978.
(43) Emmert, L. A.; Choi, W.; Marshall, J. A.; Yang, J.; Meyer, L. A.; Brozik, J. A. *J. Phys. Chem. A* **2003**, *107*, 11340−11346.

Table 3. Photophysical Data for Monomer **1b** and Polymers **2** and **3**

	THF soln					solid state		
				τ_p				
material	UV−vis λ_{max}/nm	PL λ_{max}/nm	Φ_p/%	PL/μs[a]	TA/μs[b]	UV−vis λ_{max}/nm	PL λ_{max}/nm	τ_p PL/μs
1b	341	491	0.66	0.6	0.7		499	
2	335	509	0.45	0.9 (90%)[c] 150 (10%)[c]	0.9	335	516	0.9
3	342	562	0.11	160	63	345	492	1.0

[a] Photoluminescence decay lifetime. [b] Biphasic emission decay; number in parentheses indicates relative amplitude of component. [c] Transient absorption decay lifetime.

groups in the iptycene moiety. (Since there are 4 nonconjugated aryl units/molecular unit, this band is relatively strong.) In addition, it is evident that the near-UV band in polymer **2** is broader than in **1b** or **3**. The broadening of the band in polymer **2** is believed to arise due to several factors. First, since rotation of the phenylene units with respect to the Pt−acetylide chain axis is relatively unrestricted in **2**, heterogeneity with respect to conjugation length along the chain is expected to arise. By contrast, in polymer **3**, steric interactions between the PBu_3 ligands and the iptycene moiety constrain rotation around the chain axis. This gives rise to less heterogeneity with respect to conjugation length. A second factor which could contribute to broadening of the absorption of polymer **2** may be the presence of interchain aggregates. As indicated below, the existence of polymer aggregates is suggested by the photoluminescence spectrum of **2** in solution.

Another noteworthy feature in the absorption spectrum of **3** is the presence of a weak but well-defined band extending from 375 to 430 nm. This band is believed to be due to the spin-forbidden $S_0 \rightarrow T_1$ transition. This assignment is supported by the photoluminescence excitation spectrum of the polymer obtained while monitoring the phosphorescence emission (see Supporting Information). The excitation spectrum is similar to the absorption spectrum of the polymer, and it clearly shows that the long wavelength band gives rise to phosphorescence emission. Although the $S_0 \rightarrow T_1$ transition is weak in the spectrum of monomer **1b**, it is also clear in its phosphorescence excitation spectrum (see Supporting Information). The $S_0 \rightarrow T_1$ assignment for the long wavelength absorption in **3** is also supported by the fact that the spin-forbidden $S_0 \rightarrow T_1$ absorption is observed in structurally similar Pt−acetylide systems.[44,45] The reason that the spin-forbidden absorption is more pronounced in the iptycene-substituted polymer **3** compared to **1b** is unclear.

Photoluminescence spectra of **1b**, **2**, and **3** at ambient temperature in THF solution are illustrated in the right panel of Figure 3, and emission band maxima, quantum yields, and lifetimes are listed in Table 3. The emission of the three materials is dominated by a phosphorescence band between 500 and 600 nm, but all three materials also show weak fluorescence emission in the 400−500 nm region. The fluorescence assignment for the blue emission is supported by the fact that it decays very rapidly ($\tau < 200$ ps). Although intersystem crossing is likely to be very rapid in these materials, fluorescence is still observed because the radiative rate is high.[32,45] The assignment of the longer wavelength emission to phosphorescence is supported by time-resolved emission spectroscopy (see below), which indicates its decay lifetime is >0.5 μs in each material. The phosphorescence emission maxima vary in the sequence **1b** < **2** < **3**, with the latter polymer featuring the largest Stokes shift ($\lambda_{em} = 562$ nm). The phosphorescence maxima of **1b** and **2** are similar to those observed for structurally related Pt−acetylide oligomers and polymers,[28,29,32,45] and therefore, the significant Stokes shift observed for **3** appears to be unusual in this respect. The phosphorescence band shape for **1b** and **3** is dominated by a single high-energy band (the 0−0 vibronic band), with weaker bands at lower energy. The weaker bands are believed to arise from a vibronic progression due to coupling of the excitation to high-frequency modes in the Pt−acetylide backbone and the aryl rings.[29,30] By contrast, while the emission spectrum of **2** is also dominated by the 0−0 band at 509 nm, there is a second peak with $\lambda_{max} \approx 570$ nm, which is stronger than expected for a vibronic band. We believe that this transition may be due to emission from an interchain aggregate (see below). This assignment is supported by the observation that the relative intensity of the long-wavelength band increases with increasing polymer concentration in THF solution (see Supporting Information).

Time-resolved emission experiments carried out on polymers **2** and **3** in THF solution provide more insight regarding the origin of the emission (Figure 4a,b). At very early times after laser excitation (0.5 μs), the emission of **2** is dominated by a band with $\lambda_{max} = 510$ nm, which corresponds to the high-energy band seen in the steady-state emission (Figure 3). However, this emission decays very rapidly ($\tau \approx 0.9$ μs), and at later times a considerably weaker but much longer-lived emission is observed ($\lambda_{max} \approx 573$ nm, $\tau \approx 150$ μs). Note that the weak long-lived emission corresponds to the low-energy band observed in the steady-state emission. We attribute the short-lived emission to the $^3\pi,\pi^*$ exciton and the red-shifted, long lifetime emission to a triplet aggregate arising from interchain interactions. The emission of polymer **3** decays more uniformly and on a much longer time scale compared to **2** ($\tau \approx 160$ μs). At all times following excitation the emission is dominated by the band with $\lambda_{max} \approx 562$ nm, which corresponds to the band maximum in the steady-state emission spectrum.

(44) Staromlynska, J.; McKay, T. J.; Bolger, J. A.; Davy, J. R. *J. Opt. Soc. Am. B* **1998**, *15*, 1731−1736.

(45) Rogers, J. E.; Cooper, T. M.; Fleitz, P. A.; Glass, D. J.; McLean, D. G. *J. Phys. Chem. A* **2002**, *106*, 10108−10115.

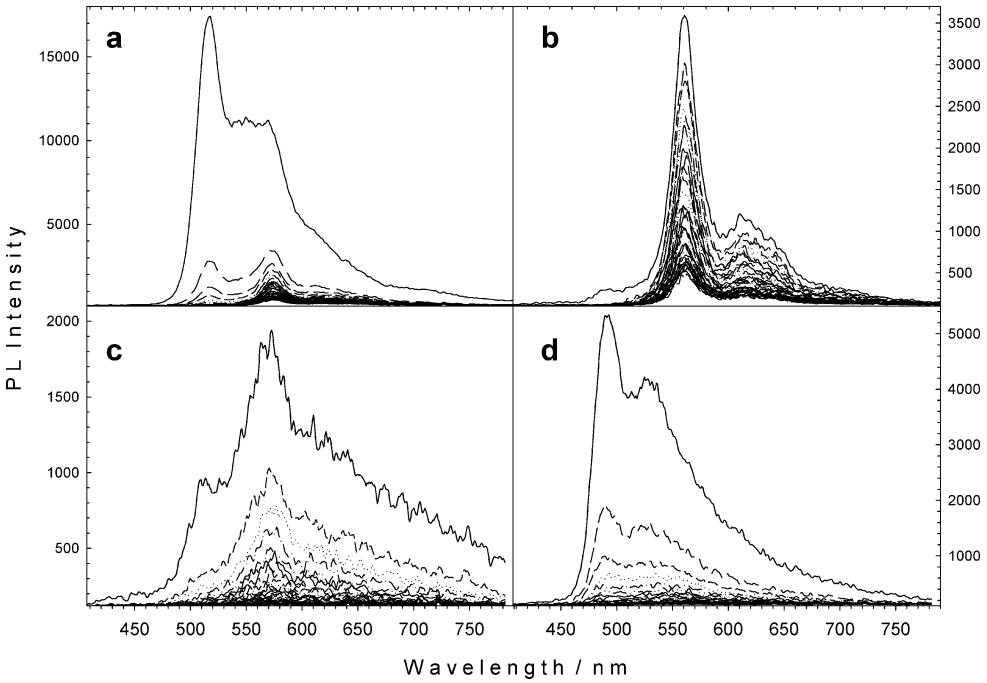

Figure 4. Time-resolved emission spectra obtained following 355 nm laser excitation: (a) polymer **2** in THF solution, $c = 0.5$ μM (delay times, 0.5−400 μs; delay increment, 10 μs); (b) polymer **3** in THF solution, $c = 1$ μM (delay times, 0.5−400 μs; delay increment, 10 μs); (c) polymer **2** spin-coated film (delay times, 0.5−40 μs; delay increment, 1 μs); (d) polymer **3** spin-coated film (delay times, 0.5−40 μs; delay increment, 1 μs).

The important point with respect to the time-resolved data is that it shows that the majority of the emission from phenylene polymer **2** decays very quickly, leaving behind a weak, long-lived emission, which we attribute to an interchain aggregate. The rapid decay is believed to occur due to quenching of the $^3\pi,\pi^*$ exciton by the interchain aggregate state. In contrast, the emission from iptycene substituted polymer **3** decays uniformly across the spectrum and considerably more slowly than **2**. We believe that the iptycene-based polymer behaves differently because the steric constraints preclude the formation of interchain aggregates which quench the intrachain exciton in **2**.

The effect of the iptycene unit on the properties of the triplet state is also manifest in the transient absorption of the polymers. Transient absorption spectra of **1b** and polymers **2** and **3** were obtained in THF solution following 355 nm excitation (Figure 5). The spectra are qualitatively similar, and they are characterized by strong bleaching of the ground-state absorption in the near-UV and transient absorption in the visible region. These spectra are similar to those observed previously for Pt−acetylide complexes which feature lowest $^3\pi,\pi^*$ excited states, and on this basis the visible transient absorption is assigned to $T_1 \rightarrow T_n$ transitions.[45,46] The transient absorptions decay with lifetimes that are in reasonable agreement with those determined by time-resolved photoluminescence (Table 3). Note that the transient decay lifetime of **3** is considerably longer than that of **2** (63 vs 0.9 μs) which reinforces the notion that the iptycene unit prevents triplet quenching due to interchain interactions.[46]

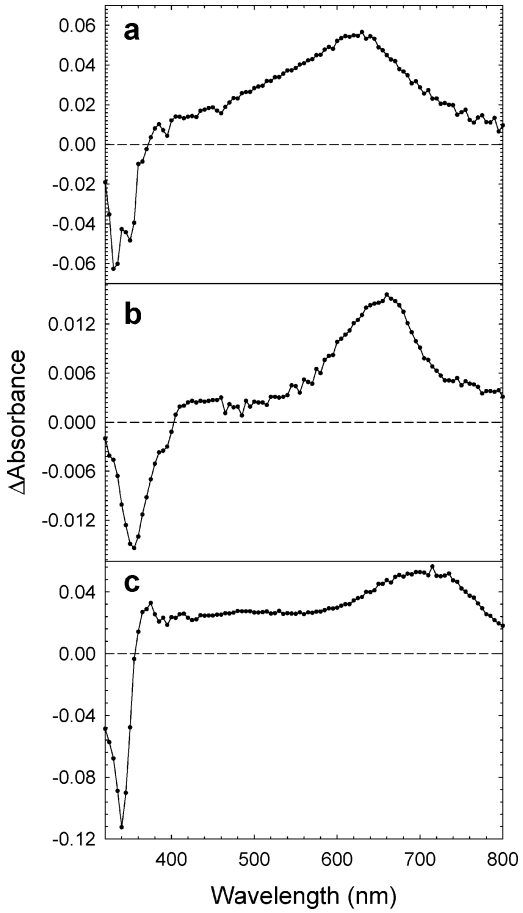

Figure 5. Transient absorption spectra obtained for samples in degassed THF solution following 355 nm excitation: (a) polymer **2**, 100 ns delay; (b) polymer **3**, 1 μs delay; (c) monomer **1b**, 100 ns delay.

Another noteworthy feature is that the triplet−triplet absorption band for **2** is considerably broader compared to that of

(46) Li, Y.; Whittle, C. E.; Walters, K. A.; Ley, K. D.; Schanze, K. S. In *Electronic, Optical and Optoelectronic Polymers and Oligomers*; Jabbour, G. E., Meijer, E. W., Sariciftci, N. S., Swager, T. M., Eds.; Materials Research Society: Warrendale, PA, 2002; Vol. 665, pp 61−72.

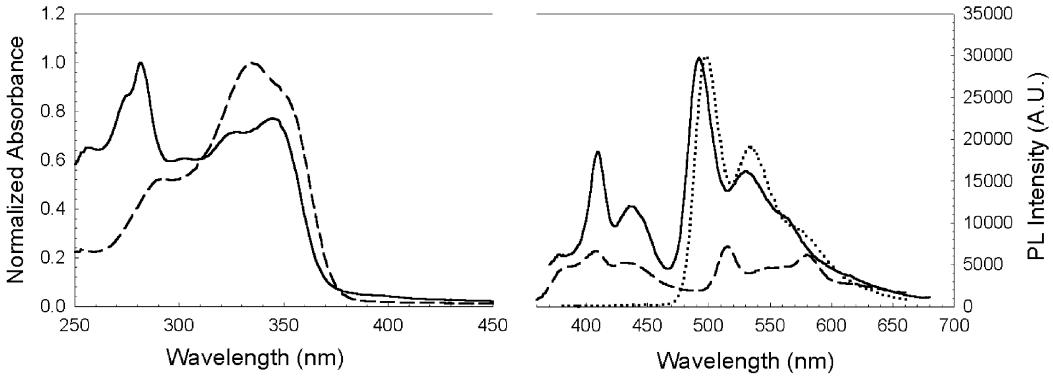

Figure 6. Absorption (left) and photoluminescence (right) spectra of spin-cast films of polymer **2** (- - -) and **3** (—) and photoluminescence of a single crystal of compound **1b** (···). The intensity of **1b** is normalized to the maximum of emission of polymer **3**. The spectra of **2** and **3** are unnormalized, and therefore, their intensities reflect the relative quantum yields for the two polymers (the spectra were obtained with films having matched absorbance).

3. This feature may also arise because there is greater conformational heterogeneity within the conjugated backbone of **2**.

Photophysics in the Solid State. The absorption and photoluminescence spectra of polymers **2** and **3** were compared as spin-coated films, while the photoluminescence of a single crystal of complex **1b** was examined. Figure 6 shows the normalized absorption spectra of the films of polymers **2** and **3**. There is no significant change in the absorption maxima compared to the solution absorbance; however, the absorption bands of both polymer films are broader compared to the solution spectra. The broadening could arise due to conformational heterogeneity in the polymer chains. Another point of note is the fact that the low-energy tail which is assigned to the $S_0 \rightarrow T_1$ transition is also evident in the solid-state absorption of **3**.

The right-hand side of Figure 6 compares the photoluminescence spectra of films of **2** and **3** and the single crystal of **1b**. The emission from the polymers was measured using films that had matched optical density at the excitation wavelength ($\lambda_{ex} = 340$ nm), and the spectra in Figure 6 are not normalized; therefore, they reflect the relative emission quantum efficiencies from the two films. Several points are of interest with respect to the solid-state emission spectra. First, the phosphorescence emission from the single crystal of **1b** and the film of **3** are very similar in energy and band shape. This feature strongly suggests that the triplet exciton in the solid state of polymer **3** experiences an environment that is very similar to that of the single crystal of **1b**. Second, the phosphorescence from **3** is considerably stronger compared to that of **2**. In addition, while the phosphorescence from **3** displays a well-defined structure, the emission from **2** is broad, and the intensities of the high- and low-energy bands ($\lambda = 516$ and 575 nm, respectively) are almost the same. Finally, it is clear that the fluorescence emission from both polymer films ($\lambda_{max} \approx 410$ nm) is nearly as efficient as the phosphorescence. This contrasts to the observations on the polymers in solution, where the phosphorescence emission was considerably more intense compared to the fluorescence. It is believed that the latter effect is likely due to the phosphorescence efficiency being lower (relative to the fluorescence) in the solid state materials, possibly due to triplet−triplet annihilation (see below).

More information concerning the photoluminescence properties of the polymer films comes from the time-resolved emission (Figure 4c,d). At early times following excitation, the emission of **2** features two bands: one at $\lambda_{max} \approx 515$ nm and a second at lower-energy with $\lambda_{max} \approx 575$ nm. The high-energy band decays quickly ($\tau \ll 1$ μs) while the low-energy band persists to longer times. Nevertheless, the overall emission from the film decays relatively rapidly with $\tau \approx 1$ μs. Interestingly, the time-resolved emission from **3** is considerably simpler. At all delay times the spectra appear much the same as the steady-state emission ($\lambda_{max} \approx 492$ nm), and the emission decays uniformly at all wavelengths with $\tau \approx 1$ μs.

In general, the photoluminescence decay lifetimes of the solid polymers are shorter than when the materials are dissolved in dilute solution. While triplet quenching by interchain aggregates may play a role in quenching of polymer **2**, given the significant reduction in lifetime observed for **3**, it is possible that triplet−triplet annihilation also plays a role in reducing the lifetime of the triplet in the films.

Aggregate Effects on the Triplet State in Pt−Acetylides. The photophysical studies presented herein indicate that interchain interactions have an influence on the properties of the triplet exciton in Pt−acetylides. In particular, the steady-state and time-resolved photoluminescence studies of **2** provide evidence for emission from an interchain aggregate, both in solution and in the solid state. The photoluminescence data on polymer **3** indicate that interchain interactions are effectively disrupted by the bulky iptycene unit. The most dramatic evidence that interchain interaction is precluded in the iptycene-substituted polymer comes from the fact that the phosphorescence of solid state **3** can almost be superimposed onto that of the single crystal of monomer **1b**.

An important question concerns the structure of the interchain aggregate(s) which give rise to the red-shifted emission observed from polymer **2** at long delay times following excitation in solution and in the solid state. It seems likely that within the aggregate the Pt−acetylide chains adopt a conformation such that the planes defined by the $Pt(PBu_3)_2(C{\equiv}C-Ar)_2$ and phenylene units are coplanar. Two or more chains in this conformation can come into close approach allowing direct $\pi-\pi$ interactions between the phenylene

residues. Although there is little in the chemical literature concerning the photophysics of triplet excimers of organic aromatic hydrocarbons,[47−50] the available evidence[47,48,50] suggests that $\pi-\pi$ interactions lead to a decrease in the T_1-S_0 energy gap as reflected by a decrease in the excimer phosphorescence energy relative to the monomer phosphorescence energy. (Note that this decrease in the phosphorescence energy could arise due stabilization of T_1 or *destabilization* S_0.) Thus, the red-shifted emission observed from polymer **2** in solution and in the solid could arise due to $\pi-\pi$ interactions which either lead to stabilization of T_1 or destabilization of S_0.

An alternate possibility is that interchain interaction in polymer **2** leads to a low-energy excited state arising from (metal−metal) d−p interactions. Specifically, it is well-established that in face-to-face dimers of d^8-d^8 metal complexes there exists a manifold of energetically low-lying excited states arising from a $d\sigma^* \rightarrow p\sigma$ transition.[35] The prototypical example of this interaction is provided by the complex $[Pt_2(\mu\text{-}P_2O_5H_2)_4]^{4-}$ (Pt−pop), which is a d^8-d^8 complex with a Pt−Pt separation distance of 2.95 Å.[35] Pt−pop exhibits phosphorescence at 514 nm from a triplet excited-state arising from the $d\sigma^* \rightarrow p\sigma$ configuration. Yam and co-workers reported a low-energy phosphorescence ($\lambda_{max} \approx 600$ nm, $\tau \approx 20\ \mu$s) from a Pt−acetylide dimer in which two *trans*-$Pt(PR_3)_2(C{\equiv}CAr)_2$ units are held in a face-to-face orientation with a Pt−Pt separation distance of ≈3.4 Å.[51] They ascribe the luminescence to a triplet state arising from a $d\sigma^* \rightarrow p\sigma/\pi^*$ configuration (where $p\sigma/\pi^*$ is an orbital having mixed Pt p and acetylide π^* character). The mixed $p\sigma/\pi^*$ character of the acceptor ligand in the Pt−acetylide dimer lowers the energy of the transition relative to its position in Pt−pop, despite the fact that the Pt−Pt separation distance is longer in the acetylide dimer.

On the basis of this work, we suggest that the low-energy aggregate emission observed from **2** may arise from a $d\sigma^* \rightarrow p\sigma/\pi^*$ state that is produced by face-to-face Pt−Pt interaction in the interchain aggregate. Although the PBu_3 groups may hinder close approach of two Pt centers, packing forces in the solid may be sufficient to overcome the steric hindrance. Importantly, the low-energy emission observed from **2** occurs at a slightly higher energy compared to the $d\sigma^* \rightarrow p\sigma/\pi^*$ emission in the face-to-face Pt-acetylide dimers studied by Yam and co-workers. This suggests that if the $d\sigma^* \rightarrow p\sigma/\pi^*$ assignment for the low-energy emission of **2** is correct, then the Pt−Pt separation distance in the aggregates is likely >3.4 Å.

Summary and Conclusion

This investigation has examined the effect of aggregation on the properties of the triplet exciton in two Pt−acetylide polymers, **2** and **3**. Parent polymer **2** features a π-conjugated backbone in which the organic repeat unit is 1,4-diethynylbenzene. The photoluminescence of this polymer in solution and in the solid state consists of two bands, and the lower energy band is believed to arise from an interchain aggregate. The photoluminescence of polymer **3**, which is structurally similar to **2** but contains a sterically demanding iptycene unit, is dominated by a single emission band, both in solution and in the solid state. The emission from **3** is believed to arise from the triplet exciton. No evidence for interchain interaction is present in the photoluminescence spectrum of **3**, presumably because the sterically demanding iptycene units prevent the Pt−acetylide chains from approaching sufficiently to allow strong interchain interaction. Interestingly, the phosphorescence of **3** in the solid state is virtually superimposable with the emission of a single crystal of iptycene-substituted monomer **1b**. The X-ray crystal structure packing diagram of **1b** shows clearly that the Pt−acetylide chains are well-separated (≈12 Å) due to the sterically demanding iptycene units. Although it is likely that the packing in the solid state of the iptycene-substituted polymer **3** is less ordered than in the crystal of **1b**, the average interchain separation distance in the solid polymer is probably similar to that of the single crystal of the monomer.

Two possible mechanisms are considered to explain the origin of the aggregate emission in **2**. The first involves stabilization of T_1 (or destabilization of S_0) due to interchain $\pi-\pi$ interactions. The second mechanism involves interchain Pt−Pt interaction leading to a manifold of low-energy excited states based on a $d\sigma^* \rightarrow p\sigma/\pi^*$ transition. Studies in progress on structurally well-defined Pt−acetylide complexes in which a 1,8-naphthalene unit is used as a scaffold to bring two Pt−acetylide chains into close proximity will hopefully provide more insight concerning the dominant mechanism for interchain interactions in this class of materials.

Acknowledgment. We gratefully acknowledge the Air Force Office of Scientific Research (Grant No. F49620-03-1-0127) for support of this work. K.A.A. wishes to acknowledge the National Science Foundation and the University of Florida for funding of the purchase of the X-ray equipment. We also express our appreciation to Prof. Timothy Swager for a sample of the diethynyl iptycene (compound **4**) which was used in preliminary synthetic work.

Supporting Information Available: X-ray crystal structure data and thermal ellipsoid plot for compound **1a**, ^{1}H NMR spectra of **1b**, **2**, and **3**, emission spectra of **2** in THF at various polymer concentrations, emission excitation spectra of **1b** and **3**, and crystallographic data for **1a**,**b** in CIF format. This material is available free of charge via the Internet at http://pubs.acs.org.

IC048961S

(47) Langelaar, J.; Rettschnick, R. P. H.; Lambooy, A. M. F.; Hoytink, G. J. *Chem. Phys. Lett.* **1968**, *1*, 563−565.
(48) Gijzeman, O. L. J.; Langelaar, J.; Van Voorst, J. D. W. *Chem. Phys. Lett.* **1970**, *5*, 269−272.
(49) Lim, E. C. *Acc. Chem. Res.* **1987**, *20*, 8−17.
(50) Yamaji, M.; Tsukada, H.; Nishimura, J.; Shizuka, H.; Tobita, S. *Chem. Phys. Lett.* **2002**, *357*, 137−142.
(51) Yam, V. W.-W.; Yu, K.-L.; Wong, M.-C.; Cheung, K.-K. *Organometallics* **2001**, *20*, 721−726.